Combustion and Flame 161 (2014) 2371–2386

Contents lists available at ScienceDirect

Combustion and Flame

journal homepage: www.elsevier.com/locate/combustflame

Transient flame–wall interactions: Experimental analysis using spectroscopic temperature and CO concentration measurements

Markus Mann[a], Christopher Jainski[a], Matthias Euler[a], Benjamin Böhm[b], Andreas Dreizler[a,*]

[a] Fachgebiet Reaktive Strömungen und Messtechnik, Center of Smart Interfaces, TU Darmstadt, Jovanka-Bontschits-Str. 2, 64287 Darmstadt, Germany
[b] Fachgebiet Energie- und Kraftwerkstechnik, TU Darmstadt, Jovanka-Bontschits-Str. 2, 64287 Darmstadt, Germany

ARTICLE INFO

Article history:
Received 2 August 2013
Received in revised form 3 December 2013
Accepted 19 February 2014
Available online 13 March 2014

Keywords:
Flame–wall interaction
CARS
CO LIF

ABSTRACT

This paper reports on simultaneous measurement of temperature and CO concentration in atmospheric methane/air jet flames impinging vertically against a water-cooled stainless-steel wall. Flame–wall interactions are investigated for statistically stationary flames and propagating flames, representing the recognized case of head-on quenching. Instantaneous temperatures are determined using nanosecond coherent anti-Stokes Raman spectroscopy of nitrogen (CARS); CO concentrations are measured using two-photon laser-induced fluorescence (LIF). Statistically stationary flames are investigated in a parametric study for equivalence ratios ($0.83 < \phi < 1.2$) and two turbulence intensities. Surface temperatures were measured using phosphor thermometry (TP). Extrapolation of the gas phase to the wall temperature allows estimation of the error in determining the wall position. For transient flame–wall interactions flames are initiated by a laser-spark 27 mm below the wall and propagate against the wall. Head-on flame quenching is studied in these cases for $0.83 < \phi < 1.0$. Quenching distances and maximum wall heat fluxes are derived from the quantitatively measured gas phase temperatures. Conditional statistics are deduced from 200 individual quenching events and are analyzed for distance from the wall. Enthalpy losses of the flame to the wall severely impact the thermo-chemical state, causing significant deviation from stationary conditions. Spatial and temporal profiles of the transient flames are also investigated. The quenching layer is found to be in the range of 0.17–0.32 mm with corresponding dimensionless quenching distances between 0.38 and 0.68. During transient flame quenching the wall heat flux is enhanced by a factor of two and reaches values ranging from 0.24 to 0.48 MW/m^2. The normalized quenching heat flux is found to be 0.29 for lean and 0.52 for stoichiometric methane/air flames. These values are in agreement with experimental studies that used very different measurement techniques and with results from direct numerical simulations (DNS) reported in the literature.

1. Introduction

Flames are quenched by solid surfaces in a range of practically relevant combustion systems. Such processes are generally termed as flame–wall interaction (FWI). FWI can be classified in fluid-mechanical, thermal and thermo-chemical aspects. Adiabatic flame temperatures typically exceed permitted operating temperatures of metal walls. Therefore, walls are cooled such that heat fluxes occur within the boundary layers. Enthalpy losses impact local thermo-chemical states. Even though FWI takes place in only a fraction of the combustion chamber, it can play a key role in the formation of pollutants, such as unburned hydrocarbons in crevices [1] or carbon monoxide (CO), as well as flame flashback [2,3]. There is a clear trend towards downsizing in automotive internal combustion engines and aircraft engines, which increases the surface-to-volume ratio, raising the importance of FWI phenomena in combustion engine design even further.

In the past decade, computational fluid dynamics (CFD) has gained importance in the design of combustion systems. Typical mesh sizes for numerical simulations are in the order of 1 mm for complex geometries [4], which is larger than the quenching region, scaling with the laminar flame thickness, as shown experimentally [5] and numerically [6,7]. Strategies utilized in CFD to handle wall-boundary conditions, such as enthalpy losses or the treatment of thermo-chemical states, need experimental data for validation even though some direct numerical simulations (DNS) aim to fulfill this function and support a basic understanding of underlying phenomena [8–11]. However, most DNS studies have massive computational costs and are limited to generic

---

* Corresponding author. Fax: +49 6151 16 6555.
E-mail address: dreizler@csi.tu-darmstadt.de (A. Dreizler).

http://dx.doi.org/10.1016/j.combustflame.2014.02.008

configurations and/or simple fuels. Transferability to practical combustion geometries is not straightforward.

Experimental investigation of flame–wall interactions is very challenging because of the small characteristic scales involved in space and time. Nevertheless, pioneering measurement of quenching distances and their dependency on fuels, composition and pressure were carried out using ion probing [12–14]. Flame luminosity measurements of quenching distances are reported for IC engines [15] and for sidewall and head-on quenching of methane/air flames in closed vessels [16]. These authors found that flame quenching is linked to high heat flux gradients in the quenching layer.

A large number of experiments were devoted to measuring heat flux in impinging flames at steady-state. An overview is provided in [17]. For FWI, a global thermal formulation was introduced by Lewis and von Elbe [18] and refined by Karman [19]. A similar formulation was used in combined transient heat flux [20] and qualitative quenching distance measurements [5,21], and DNS [6]. Several DNSs deal with more complex fuels and the formation of unburned hydrocarbons (UHC) during quenching [22,23] and in the post-flame zone [24].

Due to its non-intrusive and in situ nature, laser spectroscopy has many advantages compared to conventional probe sampling techniques. Close to solid surfaces probe techniques either fail completely by severely disturbing the flame or are not able to capture highly transient processes, such as quenching of propagating flames. In contrast to probe techniques, laser-based diagnostics provide high spatial resolution due to a well-defined probe volume that can be positioned very close to the wall. By using q-switched pulse lasers operating in the nanosecond regime, laser spectroscopy has superior temporal resolution compared to any other technique, such as luminescence imaging, as applied in other studies.

Reports of direct spectroscopic measurements of species concentration or temperatures in quenching flames are scarce. CARS measurements of temperature within the boundary layer inside an IC engine were reported by Lucht and Maris [25]. A more recent spectroscopic study of FWI was carried out by Fuyuto et al. [26], measuring mean temperature and mean intermediate species concentration of a steady-state side-wall quenching geometry. They used several LIF techniques as close as 200 μm from a cooled surface. In previous research at the Center of Smart Interfaces at TU Darmstadt the focus was on simultaneous gas phase temperature, heat flux and carbon monoxide (CO) concentration measurements in the near-wall region of stationary laminar impinging jet flames [27]. In the present approach, however, these investigations were extended to include higher Reynolds numbers and higher turbulence levels, u'/u, of up to 6–7%. Results obtained from steady-state wall-stabilized flames are taken as the starting point for the investigation of transient flame–wall interactions where the flame propagates against the wall and finally quenches in a head-on quenching geometry. The primary goal is to investigate thermochemical states that differ significantly between (statistically) stationary wall-stabilized flames and flames during head-on quenching. Using conditional statistics of instantaneous CO and temperature measurements, the impact of enthalpy losses to the wall is evaluated for near-wall CO pollutant formation based on direct measurements in quenching layers.

2. Experiment

2.1. Burner configuration and ignition system

The impinging-jet burner configuration shown in Fig. 1 is based on a design presented in Ref. [28]. The burner consists of a Morel-type nozzle [29] adjusted $H = 32$ mm below a slightly convex water-cooled stainless-steel wall. The convex wall is part of a sphere. The sphere exhibits a radius of $R_{Wall} = 300$ mm. The spherical segment is $D_{Segment} = 120$ mm in diameter and is aligned axis-symmetrically with the nozzle. This convex shape allows the use of focused point-wise laser diagnostics as close as 50–100 μm to the wall while the flow field is maintained similar to that of a stagnation point flow impinging on a flat plate.

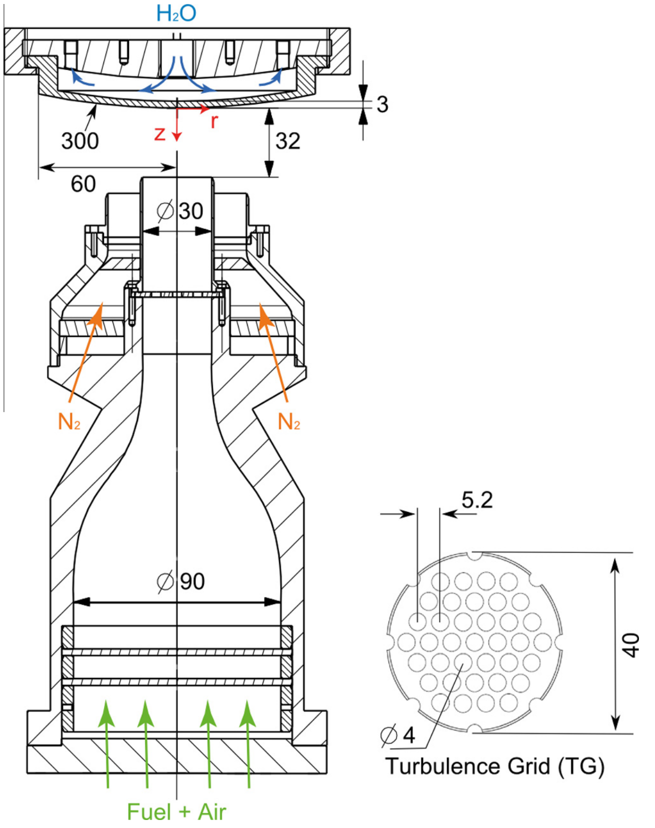

Fig. 1. Sketch of the FWI impinging jet burner. Dimensions are given in mm. Installation of the turbulence enhancing grid is optional. The entire system is mounted on an x–y–z translation stage, allowing for micrometer steps. For details see text and compare discussions in [28].

The Morel-type nozzle has an outlet diameter of $D = 30$ mm and a contraction ratio of 9 based on inlet/outlet area ratio, contracted at a length of $L_c/D_1 = 1.2$ (D_1: settling chamber diameter, L_c: contraction length). Inside the nozzle the flow is homogenized by two mesh gaskets upstream of the contraction. The optional use of a turbulence generator (TG, compare to Fig. 1) 60 mm upstream of the nozzle outlet enhances the turbulence level, u'/u, from less than 0.5% to 6–7%. Integral length scales at the nozzle exit are reduced by using the turbulence generator from ~15 mm (estimated from the half nozzle diameter) to ~4.7 mm, as deduced from auto-correlations of the axial velocity component. Auto-correlations were measured using hot-wire anemometry in a previous study [28]. The turbulence generator is a plate that is perforated with hexagonally arranged holes of 4 mm diameter and the blocking ratio is 45%. Installation of the turbulence generator enhances the pressure drop of the nozzle. Consequent separation is suppressed by two 5 mm-wide annular meshes next to the wall. These annular meshes are installed at positions 5 mm and 45 mm downstream of the beginning of the contraction. To prevent ambient air from entraining into the reaction zone, the reactive jet can be surrounded by a nitrogen coflow. The diameter of the concentric coflow nozzle is $D_{Coflow} = 60$ mm; it is staged 7 mm below the main nozzle to grant full optical access above the nozzle, as needed for